Motor Task Difficulty and Brain Activity: Investigation of Goal-Directed Reciprocal Aiming Using Positron Emission Tomography

CAROLEE J. WINSTEIN,[1] SCOTT T. GRAFTON,[2,3] AND PATRICIA S. POHL[1]
[1]*Department of Biokinesiology,* [2]*Department of Neurology, and* [3]*PET Imaging Science Center, University of Southern California, Los Angeles, California 90033*

Winstein, Carolee J., Scott T. Grafton, and Patricia S. Pohl. Motor task difficulty and brain activity: investigation of goal-directed reciprocal aiming using positron emission tomography. *J. Neurophysiol.* 77: 1581–1594, 1997. Differences in the kinematics and pattern of relative regional cerebral blood flow (rCBF) during goal-directed arm aiming were investigated with the use of a Fitts continuous aiming paradigm with three difficulty conditions (index of difficulty, ID) and two aiming types (transport vs. targeting) in six healthy right-handed young participants with the use of video-based movement trajectory analysis and positron emission tomography. Movement time and kinematic characteristics were analyzed together with the magnitude of cerebral blood flow to identify areas of brain activity proportionate to task and movement variables. Significant differences in rCBF between task conditions were determined by analysis of variance with planned comparisons of means with the use of group mean weighted linear contrasts. Data were first analyzed for the group. Then individual subject differences for the movement versus no movement and task difficulty comparisons were related to each individual subjects' anatomy by magnetic resonance imaging. Significant differences in rCBF during reciprocal aiming compared with no-movement conditions were found in a mosaic of well-known cortical and subcortical areas associated with the planning and execution of goal-directed movements. These included cortical areas in the left sensorimotor, dorsal premotor, and ventral premotor cortices, caudal supplementary motor area (SMA) proper, and parietal cortex, and subcortical areas in the left putamen, globus pallidus, red nucleus, thalamus, and anterior cerebellum. As aiming task difficulty (ID) increased, rCBF increased in areas associated with the planning of more complex movements requiring greater visuomotor processing. These included bilateral occipital, left inferior parietal, and left dorsal cingulate cortices—caudal SMA proper and right dorsal premotor area. These same areas showed significant increases or decreases, respectively, when contrast means were compared with the use of movement time or relative acceleration time, respectively, as the weighting factor. Analysis of individual subject differences revealed a correspondence between the spatial extent of rCBF changes as a function of task ID and the individuals' movement times. As task ID decreased, significant increases in rCBF were evident in the right anterior cerebellum, left middle occipital gyrus, and right ventral premotor area. Functionally, these areas are associated with aiming conditions in which the motor execution demands are high (i.e., coordination of rapid reversals) and precise trajectory planning is minimal. These same areas showed significant increases or decreases, respectively, when contrast means were compared with the use of movement time or relative acceleration time, respectively, as the weighting factor. A functional dissociation resulted from the weighted linear contrasts between larger (limb transport) or smaller (endpoint targeting) type amplitude/target width aiming conditions. Areas with significantly greater rCBF for targeting were the left motor cortex, left intraparietal sulcus, and left caudate. In contrast, those areas with greater rCBF associated with limb transport included bilateral occipital lingual gyri and the right anterior cerebellum. Various theoretical explanations for the speed/accuracy tradeoffs of rapid aiming movements have been proposed since the original information theory hypothesis of Fitts. This is the first report to relate the predictable variations in motor control under changing task constraints with the functional anatomy of these rapid goal-directed aiming movements. Differences in unimanual aiming task difficulty lead to dissociable activation of cortical-subcortical networks. Further, these data suggest that when more precise targeting is required, independent of task difficulty, a cortical-subcortical loop composed of the contralateral motor cortex, intraparietal sulcus, and caudate is activated. This is consistent with the role of motor cortex for controlling direction of movement on the basis of population encoding.

INTRODUCTION

Chronometric approaches to the study of the control of goal-directed hand aiming movements show that the precision or complexity requirements of the aiming task can be generally described through the effect that the index of difficulty (ID) has on movement time (Fitts 1954; Fitts and Peterson 1964). Movement time increases as the width of the target decreases or when the distance to the target increases. The formulation of Fitts (1954) for this linear relationship is given by the following equation

$$MT = a + b\,[\mathrm{Log}_2\,(2A/W)] \quad (1)$$

where MT is the movement time between two targets for discrete aiming or average movement time for continuous, reciprocal aiming, and a and b are empirically derived constants. In Fitts' law, the ID is represented by the term $[\mathrm{Log}_2\,(2A/W)]$, where A is the distance between the center of each target and W is the width of each target in the plane of movement. The time dependency characterizes the speed-accuracy tradeoff for rapid, goal-directed aiming movements. This highly reproducible movement time effect is in part an outcome of increasing motor planning and requisite visual feedback as task constraints increase and accuracy is maintained (Keele 1968; Meyer et al. 1988; Wallace and Newell 1983; see Keele 1986 for a review).

The brain structures where motor planning of goal-directed aiming movements occurs (as used in the Fitts paradigm) are not known. Electrophysiology studies in nonhuman primates performing directional aiming movements demonstrate population coding of movement direction in motor cortex and superior parietal cortex (Ashe and Georgopoulos 1994; Georgopoulos et al. 1986; Schwartz et al. 1988;

for review see Georgopoulos 1995). These studies have not examined neural activity in relation to a task dimension such as the ID. Previous positron emission tomography (PET) studies in humans also implicate dorsal premotor, motor, and superior parietal cortex for control of reaching, grasping, or pointing movements (Grafton et al. 1992, 1996b). These experiments are typically categorical comparisons of movement versus control/no movement. As in the electrophysiology studies, a parametric analysis in which task difficulty was the parameter of interest was not examined. A primary goal of this experiment was to determine the functional neural anatomy associated with the control of continuous goal-directed aiming movements. In addition to completing a categorical comparison of movement versus no movement, the experiment was primarily designed to examine the effect of task complexity by testing subjects at different IDs. Differences along this dimension would identify areas more involved in planning as task constraints of directed arm movements increase.

By requiring subjects to perform the Fitts task across different levels of difficulty, limb kinematics could be systematically varied (MacKenzie et al. 1987). We used high-speed video recordings to characterize the kinematics of these arm aiming movements. For the purposes of PET imaging, the Fitts aiming task was modified only slightly so that blocks of continuous, reciprocal aiming movements were executed in the vertical dimension. In a prior PET study of limb pointing (Grafton et al. 1996b) we observed a correlation of blood flow increases in motor areas with the time required to complete each reaching movement (i.e., mean limb velocity since the reaching distance was constant). However, blood flow increases in these same areas also correlated inversely with the total amount of movement made during each scan. This was because subjects that reached quickly spent more dwell time waiting for the next go cue in this task with a fixed intertrial interval. Thus a direct relationship of the kinematic parameter of interest (limb velocity) and cerebral blood flow (CBF) responses could not be established. Therefore in the current study the task was controlled so that the proportion of time with movements (and also dwell time) remained constant across all scans. Brain areas with blood flow responses proportionate to the average time to complete a reaching movement, peak velocity, number of hits, and time to peak velocity (acceleration) could then be identified. We were particularly interested to see which of these dependent measures corresponded best to CBF increases in motor areas. We did not attempt to dissociate eye and limb movements. Instead, oculomotor and limb control were treated as a unitary functional system.

A third feature of the Fitts paradigm is that the aiming task can be made more difficult by selectively increasing the movement amplitude (distance between targets) or by changing target size. The PET implementation of the reciprocal aiming task was designed so that these two types of task difficulty (amplitude vs. precision aiming) could be examined separately. Thus, under common difficulty conditions, brain areas with greater relative activity for the control of limb transport under higher-amplitude conditions could be differentiated from areas more active during precision aiming, where endpoint targeting is more critical.

METHODS

Subjects

Six right-handed (Oldfield 1971) young adults (23 ± 3.8 yr, mean ± SD; 3 male, 3 female) participated in the study after informed consent was obtained in accordance with the Institutional Review Board of the University of Southern California. All subjects were normal by medical interview.

Apparatus and behavioral task

Equipment for the aiming task included a lightweight hand-held stylus with a globe-shaped reflective marker mounted 10 mm from the tip, a millisecond timer that emitted an audible tone at the end of a trial, and a vertically mounted tapping board with metal plates distinguishing two targets, surrounded by error regions. Video recording (Panasonic AG7350) of the trajectory of the stylus was performed with a Pulnix 120-Hz video camera. A 300-W floodlamp was directed toward the stylus reflective marker during filming. Video analysis equipment included Peak Performance Technologies software and hardware with a Unipaq 386 computer interfaced with the video recorder.

The subjects held the stylus in the right hand like a pencil in a three-finger grip between the thumb, index, and middle finger pads. When verbally cued, subjects continually tapped the stylus as fast and accurately as possible alternately between the two targets for 10-s trials. There were three levels of task difficulty defined by Fitts' ID (Fitts 1954). At each ID there were two task types (i.e., amplitude/target width combinations) resulting in six aiming (movement) conditions. Amplitude/target width combinations were 10/4 and 20/8 cm for the lowest task difficulty (ID = 2.32 bits); 10/1 and 20/2 cm for the moderate-difficulty (ID = 4.32 bits); and 10/0.25 and 20/0.50 cm for the highest-difficulty (ID = 6.32 bits).

Scanning procedure

Each subject was positioned supine with the head in the scanner and the right arm free to move in a vertical direction, as shown in Fig. 1. The tapping board was mounted vertically to the right, within view and within reach of the right arm. The video camera was positioned orthogonal to the plane of movement (Fig. 1, *inset*). Movement of the stylus during each 90-s scan was filmed at a rate of 120 Hz. During each 90-s movement scan, the subject performed five 10-s continuous aiming trials interpolated with 5-s rests. A tone sounded after each 10-s trial, triggering the 5-s rest period. The experimenter prompted each subsequent trial with a verbal cue. Although a wide range of movement speeds was generated across task conditions and subjects, each movement scan included the same proportion of limb movement and rest.

Each movement scan was paired with a 90-s no-movement/control scan. During control scans the subject held the stylus tip stationary on the lower target (with the use of the same amplitude/target combination as in the paired movement scan) while visually monitoring its position. Although the primary objective of the experiment was to determine the functional anatomy of movement planning under varying task constraints (i.e., difficulty and task type), this simple no-movement planning task that required the same static positioning was chosen for the control condition in the categorical comparison.

Brain scans were performed 12 times; six movement scans (for the 6 different amplitude/target combinations) alternated with six control scans with no movement. The order of task difficulty and task type was counterbalanced. Scans were performed ≥10 min apart to allow for sufficient radioactive decay of ^{15}O.

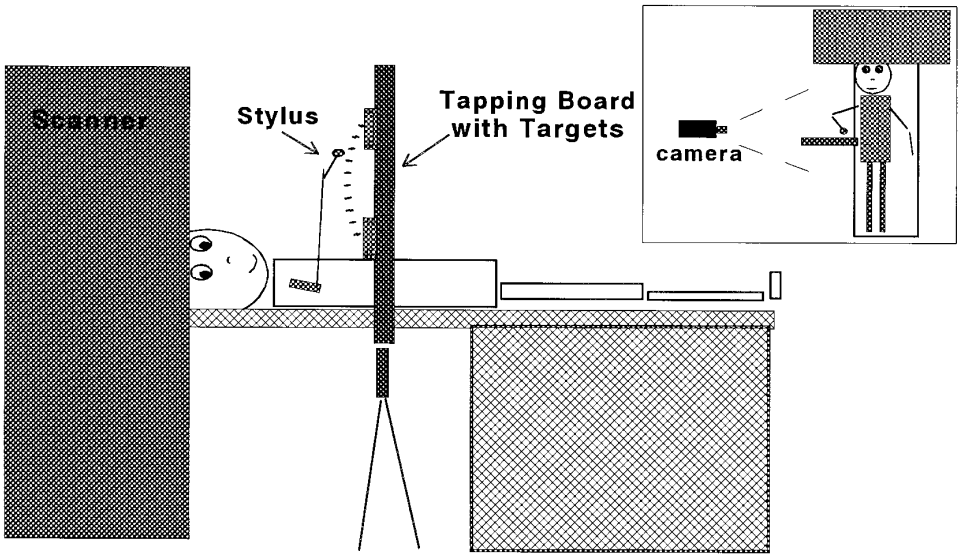

FIG. 1. Experimental setup. Subject is shown positioned supine in scanner with right arm free to aim stylus at targets positioned adjacent to and aligned vertically on the tapping board. *Inset*: video camera position for recording the 2-dimensional (sagittal) trajectory of the stylus.

Imaging

PET images of regional CBF (rCBF) were acquired with the Siemens 953/A tomograph. The device collects 31 contiguous planes covering a 105-mm field of view. The nominal axial resolution is 4.3 mm at full width half maximum (FWHM) and the transaxial resolution is 5.5 mm FWHM as measured with a line source. The tomograph was oriented 15° more steeply than the canthomeatal line, so the field of view did not include the orbitofrontal cortex.

Images of rCBF were acquired with the use of a modified autoradiographic method (Herscovitch et al. 1983; Raichle et al. 1983). A bolus of $H_2{}^{15}O$ was injected intravenously into the left arm commensurate with the start of scanning. The movement task was initiated 10 s after tracer injection. A 90-s scan was acquired and reconstructed with the use of calculated attenuation correction, with boundaries derived from each emission scan sinogram. Arterial blood samples were not obtained. Images of radioactive counts were used to estimate rCBF as described previously (Fox et al. 1984; Mazziotta et al. 1985).

Magnetic resonance imaging (MRI) of brain anatomy was available in five of the subjects. Coronal images were acquired on a General Electric Signa 1.5-T scanner with the use of a three-dimensional spoiled grass protocol (124 contiguous 1.6-mm-thick slices, TR = 3.5 ms, TE = 7 ms, flip angle 35°, 256 × 256 pixel matrix with 220-mm field of view).

Kinematics analysis

The position of the reflective marker during the three middle trials (2–4) of each movement scan was digitized and resultant two-dimensional coordinates were determined. Data were smoothed with the use of a Butterworth low-pass filter (8 Hz cutoff), and velocities were derived. Trajectory data were analyzed by cycle (liftoff to liftoff). Data from each cycle were averaged within and then across trials for each of the six task conditions to determine the number of target hits per 10-s trial, average movement time per cycle (MT), peak resultant velocity per cycle, and the percent of MT in acceleration per cycle [i.e., (time to peak velocity/cycle MT) × 100].

The study design was a 3 × 2 factorial design with separate analyses of variance (ANOVAs) used to identify the effects of three levels of task difficulty (ID) and two levels of task type (small or large amplitude/target width combination) on each dependent measure. For all F tests, significance was set at $P < 0.05$ and the Greenhouse-Geisser degrees of freedom adjustment was used to compute the probability level for the repeated measures. Post hoc linear comparisons with a Bonferroni correction were conducted to determine the loci of significant interactions.

rCBF analysis

Image processing was performed on a SUN 10-41 SPARC workstation. All rCBF images were aligned in a common stereotactic reference frame to determine a mean image for each subject. First, a within-subject alignment of PET scans was performed with the use of an automated registration algorithm (Woods et al. 1992). A mean image of the registered and resliced images was calculated for each subject. The mean PET image from each individual was coregistered to the same subject's MRI scan with the use of an automated algorithm (Woods et al. 1993a). MRI scans were then coregistered to a reference atlas centered in Talairach coordinates with the use of an affine transformation with 12 degrees of freedom (Grafton et al. 1994; Talairach and Tournoux 1988; Woods et al. 1993b). The parameters to fit were three translations, three rotations, and three rescalers oriented in a direction specified by the last three parameters. Combined registration matrices were then used to reslice all raw PET data to the final Talairach coordinate system. The resultant rCBF images were masked at a threshold of 10% of maximum; areas above this cutoff were smoothed to a final isotropic resolution of 20 mm FWHM (as verified with a line source). Previous investigations demonstrate that this magnitude of smoothing enhances signal detection (Friston et al. 1991; Grafton et al. 1990; Worsley et al. 1992). All 72 (12 scans × 6 subjects) smoothed images were normalized to each other with the use of proportionate scaling calculated from the global activity of each scan. Normalization was performed with the use of a common volume mask, to avoid global normalization errors associated with missing data.

Significant differences between task conditions were determined by ANOVA with planned comparisons of means with the use of group mean weighted linear contrasts (Neter et al. 1990; Woods et al. 1996). To account for the between-subjects variance, a randomized blocking design with subjects as a blocking effect was used for all comparisons. A t map image of significant effects was calculated on a pixel-by-pixel basis by weighting the scans as a function of a particular dependent variable of interest. Peak sites on the t map above a threshold of $P < 0.005$ were localized and maximal t and P values and mean rCBF values were tabulated for each comparison. The following six comparisons were evaluated.

MOVEMENT. A three-way ANOVA was used to identify areas demonstrating a categorical difference between directed arm movements and no arm movement with the use of all 72 scans. The three effects were task ($n = 2$, movement scans were weighted 1 vs. no-movement scans weighted -1), amplitude/target condition ($n = 6$), and subject ($n = 6$). A threshold was set at $t = 2.787$, $P < 0.005$, df = 25.

TASK DIFFICULTY. A three-way ANOVA was used to identify areas demonstrating different activity as a function of task difficulty. Only the scans during movement were used ($n = 36$). The three effects in this statistical model were ID ($n = 3$, each ID scan was weighted by the derived Fitts ID level), type of difficulty ($n = 2$), and subject ($n = 6$). A threshold was set for $t = 3.169$, $P < 0.005$, df = 10. Sites with greater or lesser CBF corresponding to task difficulty were then localized.

TYPE OF DIFFICULTY: TRANSPORT/TARGETING. A three-way ANOVA was used to identify areas more active as a function of type of difficulty. The ''type'' of difficulty referred to either the smaller (10/4, 10/1, 10/0.25 cm) or the larger (20/8, 20/2, 20/0.5 cm) amplitude/target width ID conditions. The three effects and t and P thresholds in this statistical model were the same as those used for the task difficulty comparison, except that the two task type scans were weighted -1 and 1. Sites where there were CBF changes in association with the use of relatively smaller or larger amplitude/target ratios were then localized. Sites with greater rCBF in association with smaller amplitude/target combinations correspond to areas involved in planning more precise aiming (endpoint targeting), whereas those showing greater relative rCBF in association with larger amplitude/target combinations correspond to areas more involved in limb movement (transport).

For the last three comparisons, in which kinematic variables of velocity, acceleration time, and movement time were used, separate two-way ANOVAs were used to identify areas demonstrating different brain activity as a function of each of these variables. Only the scans during movement were used ($n = 36$). The two effects in each of the three statistical models were amplitude/target combination ($n = 6$) and subject ($n = 6$). Each t map image of significant kinematic variable effects was calculated by weighting the six movement scans by the kinematically measured group mean for that variable during each of the six scans (see Table 1 for group means). A threshold was set for $t = 2.787$, $P < 0.005$, df = 25 for each of the three comparisons.

Statistical differences for individual subjects were calculated with the use of analogous ANOVAs without the subject effect. PET results were superimposed on individual subject's MRI scans and rendered in three dimensions with the use of AVS (Advanced Visualization Systems) software. A statistical threshold of $P < 0.05$ was used.

RESULTS

Movement time and kinematics

Movement time and kinematic results are summarized in Table 1 and Fig. 2 and are presented first to illustrate the degree of correlation with task difficulty (ID) and type of aiming. More importantly, these results are presented because they provide the basis for the predictions regarding the CBF data.

AIMING TASK DIFFICULTY (ID) INFLUENCES MT AND KINEMATICS IN A PREDICTABLE MANNER. As task difficulty increases (from 2.32 to 6.32 bits), average MT increases from 237 to 1,145 ms/cycle, representing approximately a fivefold change ($P < 0.003$). Individual subject MTs are presented in Table 1 to illustrate the consistency of the MT change with ID across subjects, and the between-subject variability in the rate of that change (i.e., MT/ID slope). *Subject 2* shows the largest effect of increasing task difficulty on MT, whereas *subject 1* shows the smallest.

Consistent with MT changes, as task difficulty increases, peak resultant velocity decreases from 112 to 58 $cm \cdot s^{-1} \cdot cycle^{-1}$, representing a nearly twofold reduction in speed ($P < 0.0005$). Finally, the percentage of MT spent in acceleration (time to peak resultant velocity) decreases as task difficulty increases ($P < 0.0001$). In other words, the time spent in the deceleration phase as the target is approached increases from 49% to 80%, representing an increase of >1.5-fold. Thus, as predicted by Fitts' law (Fitts 1954), MT increases linearly as ID increases ($r = 0.82$, $P < 0.0001$). Further, and consistent with previous work, percent acceleration time covaries reciprocally with ID (MacKenzie et al. 1987; Milner and Izaz 1990; Pohl et al. 1996; Winstein and Pohl 1995). Change in peak velocity also covaries reciprocally with ID, but has been shown to be more affected by changes in movement amplitude (see results below) and thus would be expected to covary negatively with movement type in this paradigm (MacKenzie et al. 1987). Therefore we predict that brain areas showing increased activation with increasing task complexity (ID) would also show activation patterns that covary positively with MT and covary negatively with percent acceleration time. Conversely, those brain areas showing increased activation with decreasing task complexity would show activa-

TABLE 1. *Kinematic variables for the group and by subject for movement time*

A/TW, cm	20/8	20/2	20/0.5	10/4	10/1	10/0.25
ID, bits	2.32	4.32	6.32	2.32	4.32	6.32
S1	239.7	354.1	777.6	191.3	441.0	790.1
S2	231.5	446.6	1,840.5	195.3	808.8	1,942.8
S3	233.7	398.1	996.5	223.3	534.7	1,001.9
S4	310.6	485.1	1,278.2	251.5	637.1	1,339.0
S5	203.8	318.0	870.6	193.4	359.8	832.3
S6	316.5	443.1	1,017.2	249.2	505.7	1,051.5
MT, ms	256.0 ± 46.3	407.5 ± 62.9	1,130.1 ± 387.0	217.3 ± 28.1	547.9 ± 158.0	1,159.6 ± 430.3
Percent Accel	51.1 ± 3.5	44.3 ± 2.4	22.2 ± 4.5	51.7 ± 3.6	36.7 ± 5.0	18.7 ± 4.4
Velocity, cm/s	137.1 ± 24.7	95.3 ± 15.0	74.7 ± 9.5	85.9 ± 9.4	45.3 ± 7.6	41.0 ± 4.3
Hits	40.3 ± 7.0	24.9 ± 4.2	9.3 ± 2.7	41.0 ± 6.0	19.4 ± 5.6	9.3 ± 2.9

Values for average movement time/cycle (MT), acceleration time/cycle (Percent Accel), Velocity, and Hits (average number of hits/10-s reciprocal aiming trial) are means ± SD. A/TW, amplitude/target width condition; ID, index of difficulty; *S1–S6* = individual subject data for average movement time/cycle by aiming condition.

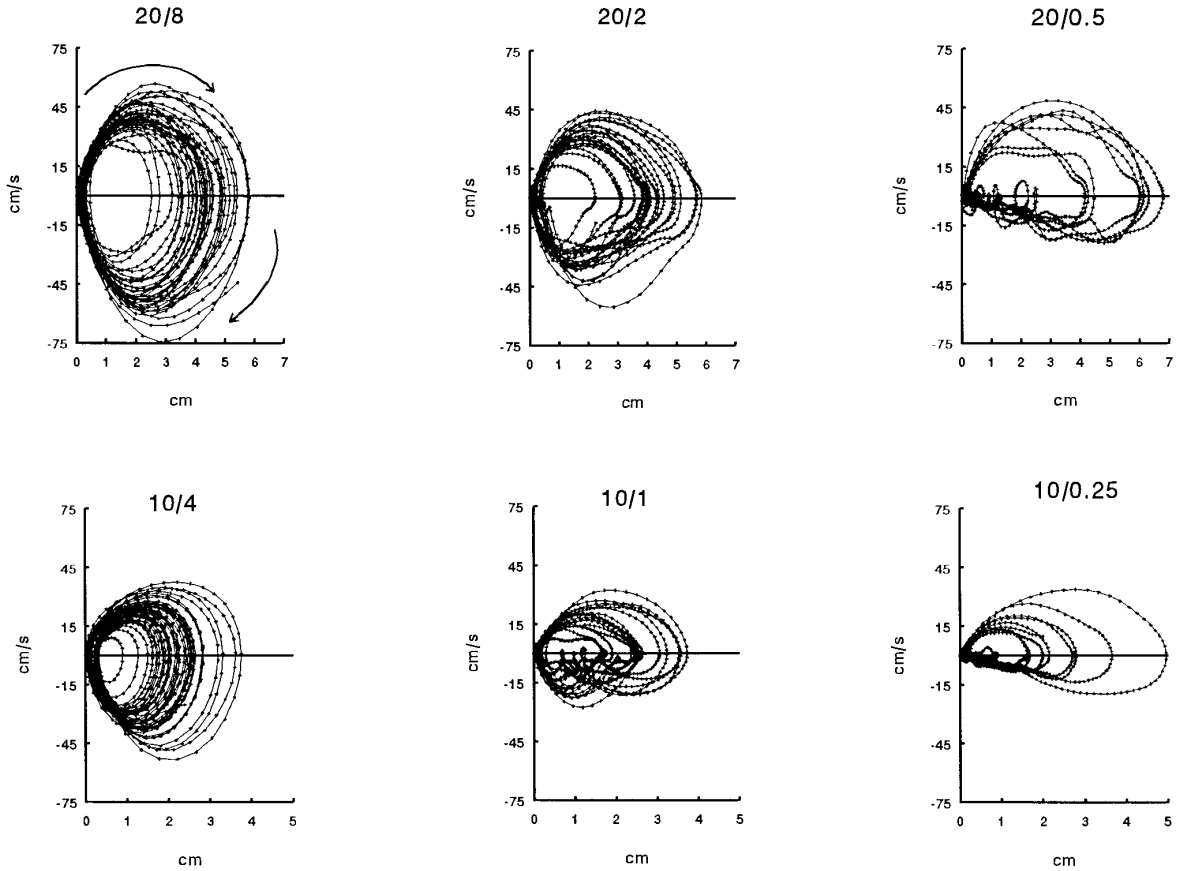

FIG. 2. Phase plane plots of horizontal position (cm) by velocity (cm/s) for 1 of each of the 10-s trials in the 6 aiming task conditions for 1 subject (*subject 4*). Labels correspond to the amplitude/target width (cm) constraints; thus plots from *left* to *right* are the 3 index of difficulty (ID) conditions (2.32, 4.32, 6.32 bits) and rows represent the task type conditions (*top*: large; *bottom*: small). Arrows in the *top left plot*: direction of movement. The trajectory above the 0-velocity line indicates movement outward away from the target ($X,Y = 0,0$) and the trajectory below the line indicates movement inward toward the target. Note the prevalence of 0-velocity crossings during the inward, homing-in phase for both high-ID condition (*right*) and the medium ID-small type condition (10/1 cm), where more precise targeting is required.

tion patterns that also covary negatively with MT and positively with percent acceleration time.

AIMING TASK TYPE INFLUENCES MT AND KINEMATICS. In contrast to the predictions of Fitts' law (Fitts 1954), there was a significant ID-by-type (small vs. large amplitude/target width) interaction such that in the 4.32 ID condition where the amplitude/target width ratios were the same, MT was longer (140-ms difference) in the small relative to the large type condition ($P < 0.04$). Similarly, in the 4.32 ID condition, the relative acceleration time in the small type condition was less (37%) than that for the large type condition (44%), thus allowing a larger proportion of MT for targeting in the deceleration phase in the small type condition. In contrast, MT and kinematic measures for the other two ID conditions at the extremes of task difficulty were not influenced by task type ($P > 0.05$). These quantitative differences can be seen qualitatively in the phase plane plots of the horizontal movement component from individual trials (Fig. 2). Data from one representative subject show obvious zero-velocity crossings during the deceleration phase in the two high-ID (6.32) conditions (*right*) and the small type medium-ID (4.32) condition (*bottom middle*). These zero-velocity crossings reflect discrete time-consuming adjustments in the trajectory during the target approach phase just before target impact.

The horizontal movement component is influenced primarily by these specific task constraints (difficulty and targeting) and not the asymmetric effects of gravity. In horizontal component phase plane plots (Fig. 2), both upper and lower targets are represented at the 0,0 coordinate. Asymmetries due to gravity would be reflected by different kinematic characteristics to the lower (gravity assisted) and upper target (against gravity). Every other movement cycle (target hit to target hit) represented as one complete circle in the phase plane would exhibit these different kinematics, such as higher velocities to the lower target. Although not evident in the horizontal movement component, these kinematic asymmetries are evident in the vertical component (not shown) corresponding to the primary movement direction.

Peak resultant velocity was systematically higher across the three ID conditions for the large type condition. This resulted in a main effect of task type ($P < 0.0001$). Across all IDs, in the large amplitude/target width aiming conditions, peak resultant velocity was nearly twice that of the small type conditions, with peak speeds of 102 cm/s com-

pared with 57 cm/s, respectively. Thus peak speed of aiming was systematically scaled as a function of task type independent of task difficulty (see MacKenzie et al. 1987 for similar findings). Therefore we predict that brain areas showing increased activation with the small (type) amplitude/target width conditions would also show activation patterns that covary negatively with peak velocity.

rCBF

MOVEMENT VERSUS NO MOVEMENT. This categorical comparison identifies brain regions demonstrating increased activity during continuous reciprocal aiming (Table 2). Consistent with previous functional imaging studies, CBF increased in well-known areas associated with the planning and execution of goal-directed arm movements (Grafton et al. 1992; Roland et al. 1982). Coregistered MRI anatomic data were available for five of the subjects. The locations of cortical activation sites with respect to local gyral anatomy in these five subjects are shown in Fig. 3. Common responses are identifiable in left sensorimotor, dorsal and ventral premotor, mesial frontal, and parietal cortex. Two sites could be distinguished in the mesial frontal area, one centered in the dorsal cingulate cortex and the other in the caudal portion of the supplementary motor area (SMA) proper. On the lateral surface, note the close proximity of responses in precentral, central, and postcentral sulci near the somatotopic arm area in all five subjects. These responses were also identifiable in a different set of subjects performing a reach and grasp task reported previously (Grafton et al. 1996b). An activation in ventral precentral gyrus or adjacent precentral sulcus (ventral premotor cortex) could be identified in four of the five subjects. Involvement of the intraparietal sulcus was less consistent, with three subjects showing relative increases in rostral intraparietal sulcus and three subjects showing increases in caudal intraparietal sulcus.

Subcortical responses included discrete blood flow increases in left putamen, globus pallidus, red nucleus, and thalamus, all components of cortical-subcortical motor circuitry (Alexander et al. 1990). As in many previous PET studies, cerebellar responses were maximal in ipsilateral anterior lobe parasagittal cerebellum. The response was large and extended into underlying cerebellar nuclei.

EFFECT OF INCREASING TASK DIFFICULTY (ID) AND RELATED KINEMATICS. Table 3, *bottom right*, summarizes the results of the *t* map contrasts that identify areas of increasing rCBF in association with increasing ID or MT. Functionally, activation in these areas is most likely associated with the visuomotor demands of aiming as accuracy constraints are increased. When contrast means were compared with the use of ID as the weighting factor, there were significant increases of rCBF in bilateral occipital (fusiform gyri), left inferior parietal, and left mesial frontal cortex, and right dorsal premotor areas (Fig. 4, *top*). The mesial frontal response extended into both the dorsal cingulate cortex and caudal SMA proper. Because separate maxima could not be identified in these two sites, this activation is described as the dorsal cingulate/caudal SMA proper site. The results from the individual subject analysis of the ID effect are shown in Fig. 5. The right premotor and left dorsal cingulate/caudal SMA proper activations could be readily identified in four of five subjects and the rostral inferior parietal activations could be localized in five of five subjects.

TABLE 2. *Movement-related brain areas during reciprocal aiming*

Region	Talairach Coordinates			rCBF, ml/min per 100 g			
	X	*Y*	*Z*	Move	Hold	*t*	*p*
L mesial frontal cortex (6)							
Caudal SMA proper	−7	−22	58	66.7	63.1	11.83	1.0E-08
L precentral sulcus (6)							
Dorsal premotor	−30	−25	57	61.2	57.4	10.39	1.0E-08
L superior parietal lobule (40/7)	−28	−48	52	59.5	62.5	6.61	1.9E-06
L central sulcus (4)							
Sensory-motor cortex	−36	−30	51	67.0	61.5	14.22	1.0E-08
L dorsal cingulate cortex (24)							
Cingulate motor area	−7	−24	48	62.9	59.8	8.93	3.0E-09
L dorsal parietal cortex (7)	−19	−70	43	55.2	58.4	5.99	7.4E-06
L precentral gyrus (6)							
Ventral premotor	−55	−7	25	45.0	42.9	6.77	4.3E-07
R superior temporal sulcus (22)	60	−45	13	40.9	38.5	6.20	1.7E-06
L thalamus (lp)	−19	−21	13	52.3	50.1	5.62	7.6E-06
L superior temporal sulcus (22)	−40	−39	12	64.9	62.2	6.00	2.9E-06
R thalamus (vl)	12	−16	12	62.3	60.1	5.47	1.1E-05
L putamen	−25	−4	10	70.2	68.8	3.90	6.4E-04
L globus pallidus	−21	−10	4	62.9	61.4	4.02	4.7E-04
L inferior temporal gyrus (37)	−39	−69	1	57.1	54.8	7.26	1.3E-07
L lingual gyrus (18)	−7	−75	0	70.0	66.1	11.19	1.0E-08
L red nucleus	−10	−22	−3	59.8	57.8	5.24	2.0E-05
R midbrain-tegmentum	1	−25	−7	61.0	59.2	5.90	3.7E-06
R fusiform gyrus (19)	39	−69	−7	51.6	49.8	4.88	5.1E-05
R anterior cerebellum	4	−55	−12	70.2	62.0	11.41	1.0E-08

Localization of movement-related areas are shown in Talairach coordinates (Talairach and Tournoux 1988). Values in parentheses are corresponding Brodmann's areas as defined by the atlas. Significance was determined with a 3-way analysis of variance and weighted linear contrasts (see text for details). rCBF, regional cerebral blood flow; SMA, supplementary motor area.

Figure 5 also shows a remarkable variation in the spatial extent of rCBF differences. Qualitatively, the rCBF responses were greatest in *subject 2* (Fig. 5, *row 2*). As shown in Table 1, this subject had relatively longer movement times, particularly in the middle- and high-ID conditions. We also observed this subject to have more difficulty executing the task than others during the PET procedure. The findings could be interpreted as showing an effort effect, such that subjects with greater difficulty in performing a more difficult task recruit greater rCBF in motor association areas.

As predicted, these same areas showed significant increases of rCBF when contrast means were compared with the use of MT as the weighting factor (excepting the left dorsal cingulate/caudal SMA proper area). When contrast means were compared with the use of acceleration time (%) as the weighting factor, there were significant decreases of rCBF in most of these same areas, reflecting the associated increase in deceleration time (%) as task difficulty and visuomotor demands increased (see Table 3, *bottom left*). This group of sites included an activation in left mesial frontal cortex, in a more rostral portion of the SMA proper. In most cases, the pattern of activation when peak velocity was used as the weighting factor was similar to that for acceleration time (%), with the following exceptions: right mesial frontal cortex, left dorsal premotor cortex, left frontal gyrus, and left intraparietal sulcus. The mesial frontal site in this case was located rostral to the vertical axis centered on the anterior commissure. This axis defines an approximate boundary of the human SMA (Zilles et al. 1996). The cortex anterior to the axis has been termed ''pre-SMA'' (Picard and Strick 1996; Tanji 1994). These four areas showed changes in rCBF only with respect to peak velocity of these aiming movements.

EFFECT OF DECREASING TASK DIFFICULTY (ID) AND RELATED KINEMATICS. Table 3, *top right*, summarizes the results of the *t* map contrasts where decreasing ID was associated with significant increases in blood flow. There were significant increases in right anterior cerebellum, left middle occipital gyrus, and right ventral premotor areas (Fig. 4, *bottom*). As predicted, these same areas showed significant increases of rCBF when contrast means were compared with the use of MT as the weighting factor. Functionally, activation in these areas is associated with aiming where the motor execution demands are relatively high (e.g., rapid reversals; see below), the trajectory planning demands are minimal, and the task requires the coordination of rapid alternating movements without the kind of visuomotor integration required of precise targeting.

As predicted, when contrast means were compared with the use of acceleration time (%) as the weighting factor, there were significant increases of rCBF in most of these same areas, reflecting the associated decrease in deceleration time (%) as task difficulty and visuomotor demands decreased (see Table 3, *top left*). In most cases, the pattern of activation when peak velocity was used as the weighting factor was similar to that for acceleration time (%), with the following exceptions: right lingual gyrus, left superior temporal sulcus, and left inferior occipital gyrus. These three areas showed changes in rCBF only with respect to peak velocity of aiming movements.

TARGETING VERSUS LIMB TRANSPORT. Fitts' law (Fitts 1954) predicts that aiming movements performed under conditions with the same amplitude/target width ratio should exhibit the same MTs, but no predictions are made about requisite motor planning and associated neural activation patterns. Our experimental design allowed us to dissociate planning related to limb transport from that related to endpoint targeting across the range of IDs. Table 4 summarizes the results of the weighted linear contrasts, showing areas with CBF changes in association with larger (limb transport) or smaller (endpoint targeting) type amplitude/target width combinations. Areas that showed significantly greater activity with limb transport included bilateral occipital lingual gyri and the right anterior cerebellum. In contrast, the three areas with significantly greater activity for end reach targeting were located in the left motor cortex, left intraparietal sulcus, and left caudate. These cortical areas are illustrated in relation to local gyral anatomy in Fig. 6.

DISCUSSION

The control of rapid target-directed movements has been of interest since before the time of the well-known review by Woodworth (1899), which describes the speed-accuracy tradeoffs in a variety of aiming tasks. Although movement scientists have long known that movement time depends both on the distance moved and on the endpoint precision as demanded by the size of the target, it was Fitts (1954) who was the first to formally define this relationship in terms of information capacity in closed systems (see Kelso 1992 for recent perspectives). Numerous mathematical and theoretical explanations for Fitts' law have been offered since its inception, including the iterative-corrections model (Crossman and Goodeve 1983; Keele 1968), the impulse variability model (Schmidt et al. 1979), the optimized initial impulse model (Meyer et al. 1988), the vector-integration-to-endpoint (VITE) model (Bullock and Grossberg 1988), and, most recently, the kinematic model based on a log-normal law (Plamondon 1995a,b). Although each new theoretical explanation has provided a more parsimonious and valid account of the mechanisms underlying the speed-accuracy tradeoff, the empirical law has survived the test of time across a variety of different aiming tasks, environmental conditions, and subject populations. Here, in our experimental design, we have used Fitts' law, the continuous aiming paradigm on which it was based, and the dimension of task difficulty as indexed by ID to identify brain areas involved in the planning of goal-directed limb movements. As Jeannerod (1994) recently argued, ''Fitts' law seems to pertain, not to the execution stage of movements (as this classical explanation would hold), but to the preparation stage. . . . The relation between duration and accuracy would thus result from neural coding of the movement during the preparatory stage. . . .'' (p. 196).

A major goal of functional imaging studies has been to identify brain areas involved in the planning of limb movements. The methodological constraints of functional imaging have limited planning experiments to imagined movements (e.g., Decety et al. 1994) and movement selection tasks (e.g., Deiber et al. 1991). The former assumes that the explicit operation of imagining movements is analogous to the

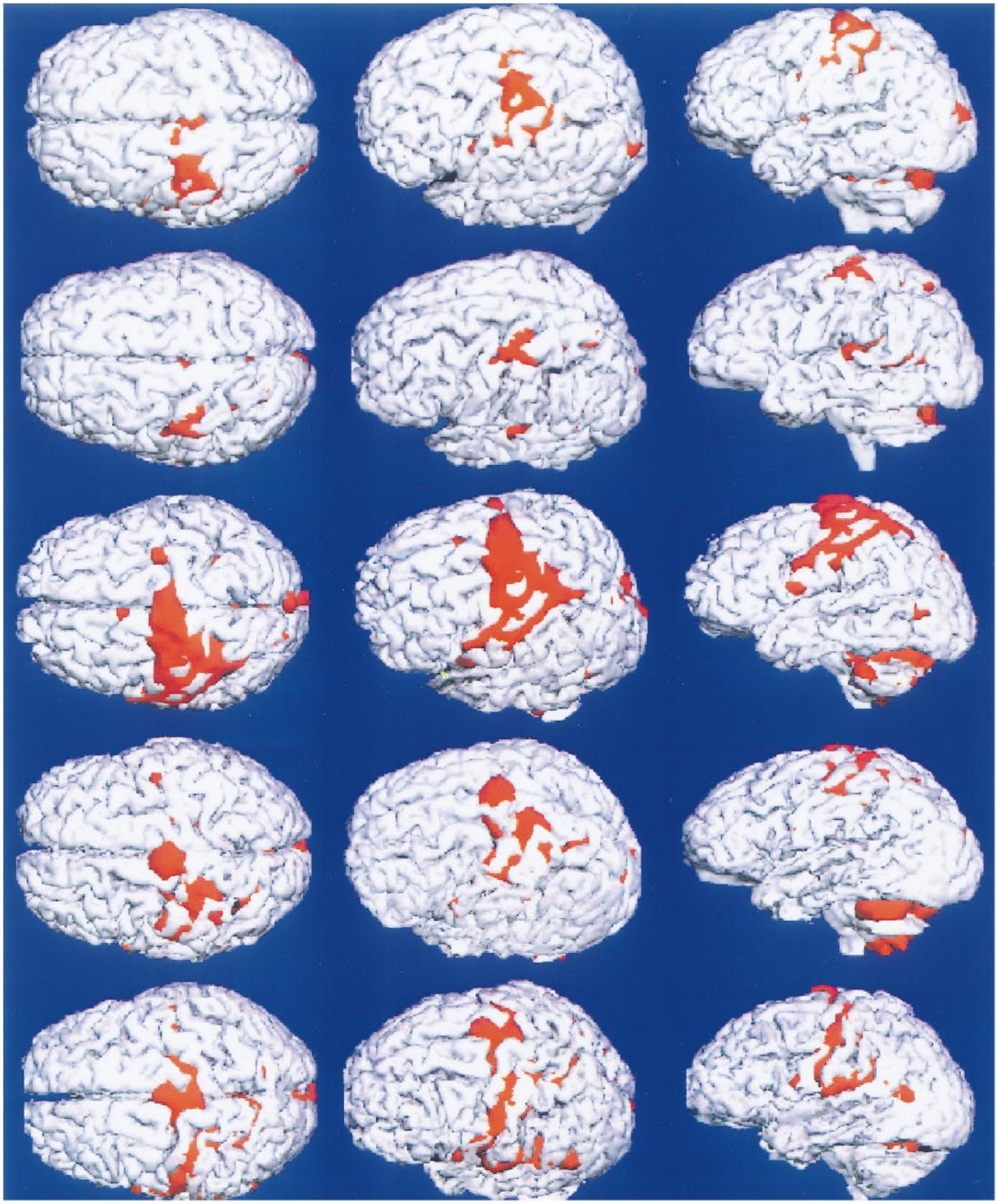

TABLE 3. *Task difficulty and kinematic related changes in brain activity*

Region	Talairach Coordinates			Significance of Kinematic Parameter (*t*-Test)			
	X	*Y*	*Z*	Acceleration	Velocity	ID	MT
R precentral gyrus (6)							
Ventral premotor	60	−3	20	9.6	10.0	−8.7	−9.4
L middle occipital gyrus (18)	−18	−87	8	9.2	7.3	−7.8	−8.8
R lingual gyrus (19)	2	−56	5		5.8		
L superior temporal sulcus (21/22)	−64	−13	−2		7.3		
R middle temporal gyrus (37)	63	−53	−4	6.0			−5.8
L lingual gyrus (18)	−3	−76	−8	7.7			−8.4
R anterior cerebellum	6	−47	−14	11.2	14.3	−10.7	−10.0
L inferior occipital gyrus (19)	−48	−81	−16		8.3		
R superior frontal sulcus (6)							
Dorsal premotor	24	−11	64	−6.2			6.4
L mesial frontal cortex (6)							
Rostral SMA proper	−3	−2	58	−9.3			9.3
R mesial frontal cortex (6)							
Pre-SMA	8	10	56		−11.3		
R superior frontal gyrus (6)							
Dorsal premotor	16	14	56	−8.1		6.0	7.6
L superior frontal gyrus (6)							
Dorsal premotor	−19	−4	55		−6.1		
L mesial frontal cortex (6/24)							
Dorsal cingulate–caudal SMA proper	−1	−10	47			6.4	
L middle frontal gyrus (6/8)	−36	15	42		−5.9		
L inferior parietal lobule (40)	−52	−44	31	−9.2		8.5	9.9
L intraparietal sulcus (7/40)	−30	−62	27		−8.7		
L caudate	−6	17	15	−6.3	−7.4		6.1
R fusiform gyrus (18)	19	−97	−10	−10.0	−9.4	10.8	9.2
L fusiform gyrus (18)	−27	−91	−16	−12.1	−12.1	11.7	11.7

Brain areas demonstrating changes in blood flow in correspondence with kinematic movement parameters. Localization in mm with respect to the anterior commissure of the midline as defined by Talairach and Tournoux (1988). Brodmann areas as defined in Talairach and Tournoux (1988) atlas coordinates are shown in parentheses. Acceleration is derived from the group average time to peak velocity normalized to movement time. Velocity: group mean peak resultant velocity of arm movements. ID, index of difficulty as defined by Fitts (1954); MT, group average movement time/cycle of the reciprocal aiming task. For other abbreviations, see Table 2. Values under movement parameters are the *t* statistic obtained in a planned comparison of contrast means in which rCBF scans were weighted by the kinematic parameter (or ID) of interest. Positive *t* statistics identify brain areas where increasing movement parameter (or ID) corresponds to increasing rCBF. Negative *t* statistics identify brain areas where decreasing movement parameters (or ID) correspond to increasing rCBF. *t*-Test cutoff: $P < 0.005$, df = 25.

planning of normal movements (which are typically performed without conscious thought). The latter experiments typically require working memory by subjects to retain conditional stimulus response maps. Again, this is a thoughtful process that diverges from the automatic and implicit planning of normal movements (see Jeannerod 1994 for recent discussion). Our experimental design identifies brain areas involved in motor planning under different levels of difficulty in a primarily procedural (implicit) task that requires little declarative (explicit) cognitive processing.

When the arm and hand are moved in free space under conditions with defined spatial constraints, as in reaching, pointing, tracking, and grasping, there is an increase in brain activity, as measured by PET, in a well-known distributed network of cortical and subcortical regions including the contralateral primary sensorimotor, premotor, caudal SMA proper, dorsal cingulate, parietal, and dorsal occipital cortices. Our categorical comparison of the activation patterns in the no-movement control versus movement conditions revealed a pattern of cortical activation consistent with that of previous functional imaging experiments with humans (e.g., Grafton et al. 1996b; Rao et al. 1993) and neurophysiological recordings in nonhuman primates (e.g., Alexander and Crutcher 1990; Fu et al. 1993; Riehle and Requin 1989; Rizzolatti et al. 1987). A new finding was an activation in ventral premotor cortex. This may be a putative homologue of area ''F4'' in monkeys (Rizzolatti et al. 1987). Neurons in F4 are particularly active during reaching movements. Activation of subcortical regions including the putamen and globus pallidus has been inconsistently seen in previous PET

FIG. 3. Movement vs. no movement. A categorical comparison of all movement scans with no-movement control scans was performed for each subject separately. Rows correspond to *S1–S5* of Table 1. Pixels reaching a threshold of $P < 0.05$ are displayed in red in 3 dimensions on the same subject's coregistered magnetic resonance imaging (MRI) scans. For all subjects, the superior views (*left*) localize responses in the inter hemispheric fissure [caudal supplementary motor area (SMA) proper]. Across all subjects there is consistent activation of the central sulcus and adjacent pre- and postcentral sulcus in the somatotopic region of the arm area of motor cortex, best seen on the left superior oblique views (*middle*). Additional activations are noted in the superior parietal lobule for all subjects. The lateral views (*right*) identify an inferior precentral gyrus/sulcus response (ventral premotor cortex) in *subjects 1, 3,* and *5.* Lateral occipital responses can also be identified in the same subjects.

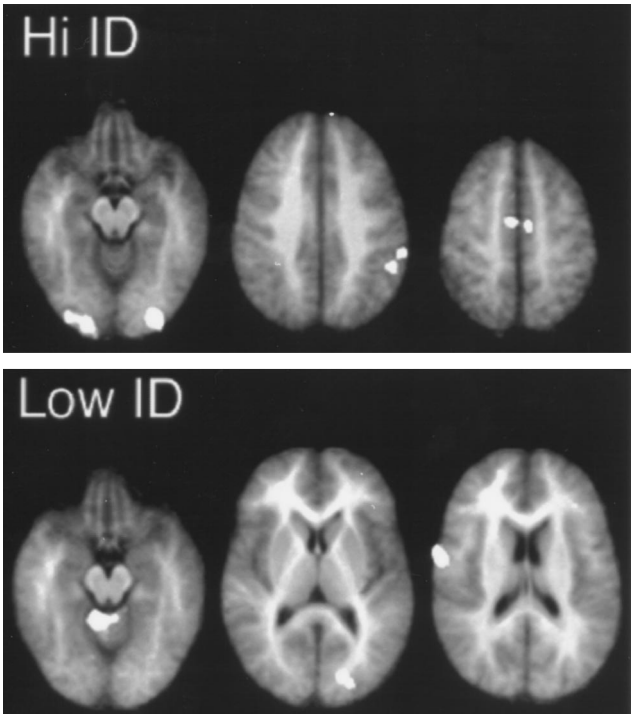

FIG. 4. Functional anatomy of Fitts' ID. *Top*: brain areas with greater activity during performance of reciprocal aiming under a greater ID. Differences are present in bilateral occipital cortex (*left*, $Z = -10$ mm), left parietal cortex (*middle*, $Z = 34$ mm), and cingulate cortex (*right*, $Z = 46$ mm). *Bottom*: brain areas with greater activity during performance of the reciprocal aiming under a lower ID. Differences are present in right anterior cerebellum (*left*, $Z = -12$ mm), left dorsal occipital cortex (*middle*, $Z = 8$ mm), and right inferior precentral gyrus, ventral premotor cortex (*right*, $Z = 18$ mm). Positron emission tomography (PET) results ($P < 0.005$) are superimposed on a population average MRI atlas in Talairach coordinates.

experiments during goal-directed aiming movements. These responses are typically small in size and magnitude. With the greater ''signal averaging'' from a large number of trials in the present experiment, these sites could be readily identified. This is consistent with neurophysiological data from nonhuman primates (Alexander et al. 1990; Georgopoulos et al. 1983) implicating a motor circuit involving a cortical-subcortical network. Of further importance to an understanding of motor planning and the neural coding associated with changes in aiming task difficulty is that a different activation pattern emerges when comparisons are made within the movement conditions.

Previous behavioral work in which a discrete Fitts aiming task was used has indicated that as task difficulty increases, more errors are made in no-vision conditions only for aiming with a task ID $\geq$4.58 bits (Wallace and Newell 1983). These results have been interpreted as evidence for the use of visual feedback for accuracy as ID increases. Further, this visual feedback time has been used to account for the prolongation in MT as ID increases. However, the task difficulty/MT relation has been demonstrated even in aiming conditions when vision is not allowed, suggesting that the increase in MT with ID is more a consequence of the motor plan than visual feedback processing time (e.g., Meyer et al. 1988; Prablanc et al. 1979; Schmidt et al. 1979). Our activation pattern associated with increases in ID seems to support both arguments. First, we see a pronounced increase in bilateral fusiform gyrus (Brodmann's area 18) activation, suggesting an increase in visual information processing as ID increases. These visual areas are most likely at the origin of a dorsal route linking striate areas to posterior parietal (contralateral inferior parietal) areas known to be involved in visual-spatial integration for action (Goodale et al. 1991; Taira et al. 1990).

In addition, the dorsal cingulate/caudal SMA proper area showed increased activation as ID increased. Although this site showed increasing CBF as task difficulty increased, it did not show the covariation with changes in MT or percent acceleration time. This suggests that the dorsal cingulate/caudal SMA proper is associated with more global planning than the kinematics of trajectory planning. In direct contrast, the left rostral SMA proper and right dorsal premotor areas showed an activation pattern that covaried with MT (positively) and percent acceleration time (negatively), without any relation to changes in task difficulty per se. Further, the right pre-SMA area showed an activation pattern that covaried (negatively) only with peak velocity. These three areas of mesial frontal cortex present with clearly unique patterns of activation with this aiming task and suggest dissociable roles in motor planning. Generally, these results are consistent with and complement other recent work showing that SMA is more active as motor task complexity increases along with requisite motor planning (Deiber et al. 1991; Grafton et al. 1992; Orgogozo and Larsen 1979; Remy et al. 1994; Shibasaki et al. 1993). Furthermore, the dorsal cingulate/caudal SMA proper, rostral SMA proper, and pre-SMA sites have also been shown to have different activation patterns for real, imagined, and observed movements (Grafton et al. 1996a; Stephan et al. 1995; Tyszka et al. 1994). The more rostral areas are associated with imagined movements, whereas the caudal areas are associated with real movements.

A comparison of the ID effect on blood flow changes across individual subjects revealed a fascinating, albeit preliminary finding. The subject with the greatest difficulty at performing the aiming task at the higher ID conditions also showed the greatest change of blood flow across ID conditions. A possible explanation is that greater effort in performing a difficult task recruits more motor planning areas. This has serious implications for interpretation of

FIG. 5. Individual subject differences in cerebral blood flow (CBF) for increasing task difficulty (ID). Areas showing greater regional CBF (rCBF) as a function of increasing ID are shown in red on the same subjects' MRI scans. *Left*: superior view; arrows indicate location of right premotor cortex response identifiable in 4/5 subjects. *Middle*: left superior oblique view; significant response is seen in the left ventral premotor cortex in *subjects 1* and *2;* however, this site was not significant in the more stringent group analysis. *Middle* and *right* (left lateral view) demonstrate in all 5 subjects a consistent response located in the left rostral inferior parietal lobule (indicated by blue arrows in *right*). There is a disparity in the relative spatial extent of the rCBF differences across subjects. rCBF changes in *subject 2* (*row 2*) are qualitatively larger than all of the other subjects. This subject had the greatest difficulty in performing the reciprocal aiming task (particularly in the higher-ID conditions).

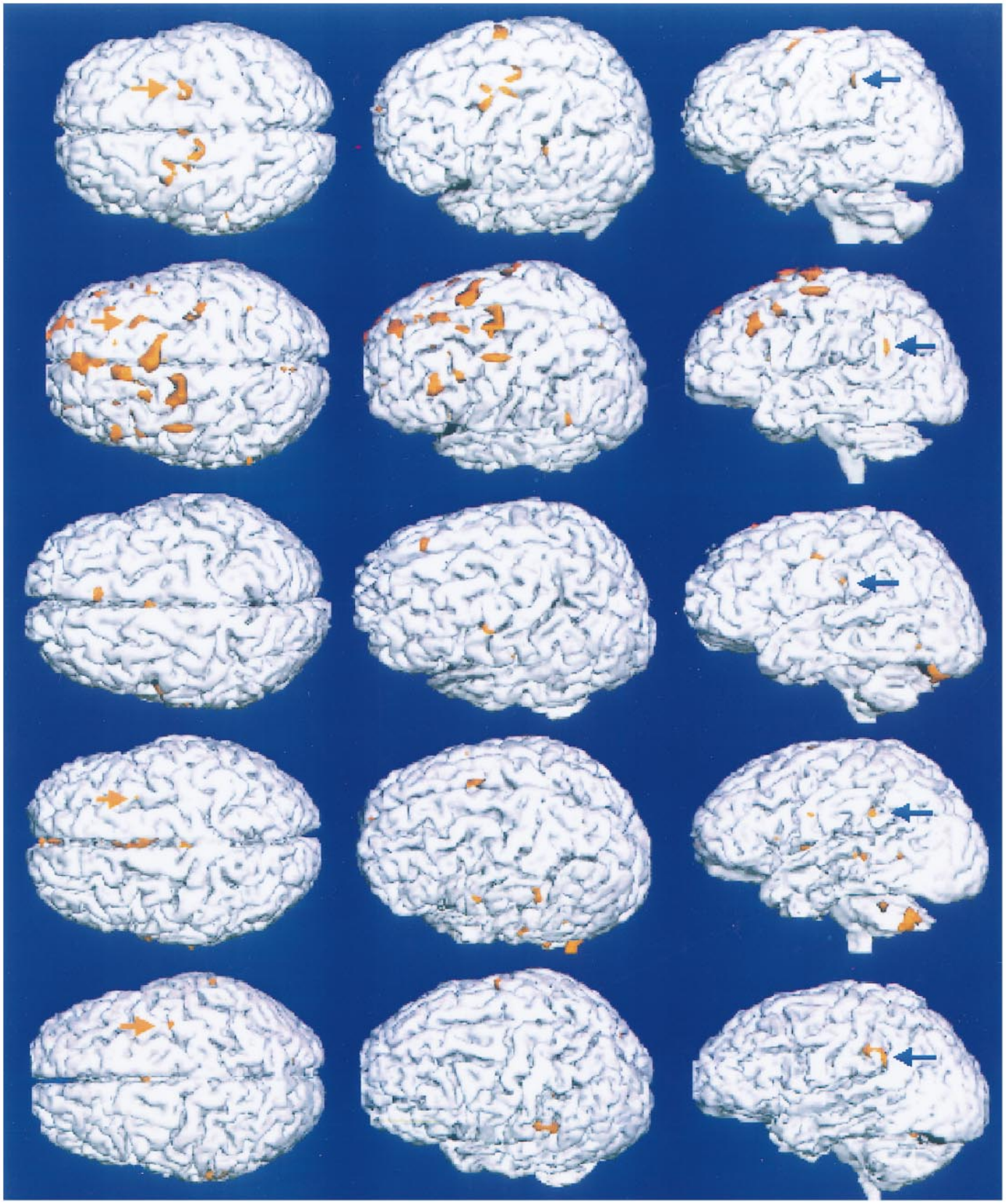

TABLE 4. *Localization of brain areas processing transport and targeting*

Region	Talairach Coordinates			Type of Aiming
	X	*Y*	*Z*	*t*-Test
Limb transport				
R lingual gyrus (19)	2	−56	5	6.0
L lingual gyrus (19)	−20	−57	−1	6.0
R anterior cerebellum	6	−47	−14	7.7
Endpoint targeting				
L central sulcus (4/motor)	−26	−21	37	6.1
L intraparietal sulcus (7/40)	−30	−62	27	6.6
L caudate	−6	17	−15	6.0

Brain areas demonstrating changes of blood flow in correspondence with the type of movement difficulty. Localization in mm with respect to the anterior commissure at the midline as defined by Talairach and Tournoux (1988). Brodmann areas as defined in Talairach and Tournoux (1988) atlas are shown in parentheses. Values are *t* statistics obtained in a planned comparison of contrast means in which rCBF scans were weighted by the type of difficulty after controlling for the ID effect. Differences in rCBF correspond to brain areas with more activity for movements with greater amplitude (limb transport) and areas with more activity for smaller target widths (endpoint targeting). For abbreviations, see Table 2.

imaging studies of recovery after stroke, where increased activity could be related to effort rather than functional reorganization.

When requisite motor planning is presumed to diminish as task ID decreases, the locus of cortical and subcortical activation shifts away from the more dorsal premotor areas to an ipsilateral ventral premotor, contralateral middle occipital, and ipsilateral anterior cerebellar activation pattern. The powerful activation of the cerebellum as task difficulty decreases is interesting when considered along with the concomitant changes in movement variables including increased acceleration time, peak velocity, and decreased MT. With this combination of movement variables, the task demands for dealing with intersegmental dynamics of the freely moving limb are naturally higher (Schneider et al. 1989; Smith and Zernicke 1987) even though the task demands for dealing with aiming accuracy are lower. Recent work with individuals with cerebellar disease suggests a role for the cerebellum in generating feedforward signals to adjust for interaction torques during reaching movements (Bastian et al. 1996). Previous recordings of dentate neurons in nonhuman primates during an alternating target aiming task before and after temporary dentate cooling showed a decrease in continuous movements and inadequate modulation of force (Brooks et al. 1973). Examination of the phase plane plots for the low-ID conditions (Fig. 2, *left*) reveals a remarkable predominance of continuous movement trajectories exhibiting pendular dynamics, with only two velocity crossings at peak outward displacement and target hit. Altogether, this suggests that the task demands in this low-ID condition are those for which the cerebellum and its unique cortical and deep nuclear circuitry is particularly suited. Of course, we cannot rule out the possibility that in the low-ID conditions the demands for continuous sensory updating might be higher than in the high-ID conditions. Recent proposals regarding the role of the cerebellum in the acquisition of sensory data (proprioceptive and cutaneous) cannot be ruled out from the present findings (Bower 1997).

Up to this point in the discussion, we have focused on the effect of task difficulty as indexed by ID. Because kinematic parameters covary with ID (i.e., movement time, peak velocity, average velocity, and % acceleration time), it is possible that the changes we see in rCBF are related to these nondissociable parameter changes and not ID per se. However, this study was designed to examine ID effects together with correlated kinematic parameters. Future studies, specifically designed to examine the isolated effects on CBF of certain kinematic parameters, such as movement velocity, are needed for a more complete understanding of the functional neuroanatomy of motor control.

When ID was controlled and brain activity was compared between the two types of aiming movements, an interesting dissociation emerged. In contrast to the predictions of Fitts' law, when the aiming task requires shorter-amplitude movements with more precise endpoint constraints (independent of ID), the increased activity in the dorsal parietal area (left intraparietal sulcus) and left central sulcus (motor cortex) reflects a distinct pattern of activity most likely associated with the enhanced targeting demands. Evidence for this is provided by the horizontal phase plane analysis. Recall that two of the three small type task conditions elicit these precise targeting adjustments, in contrast to only one of three in the large type task condition. This interpretation is consistent with results from anatomic and physiological studies in nonhuman primates that have provided substantial information regarding the central correlates of motor control. Results suggest that although cells in the primary motor cortex are predominantly active during movement and approximately one third have muscle-related properties, the majority of these cells reflect directional (load independent) effects (population coding) or effects of visual signals guiding the

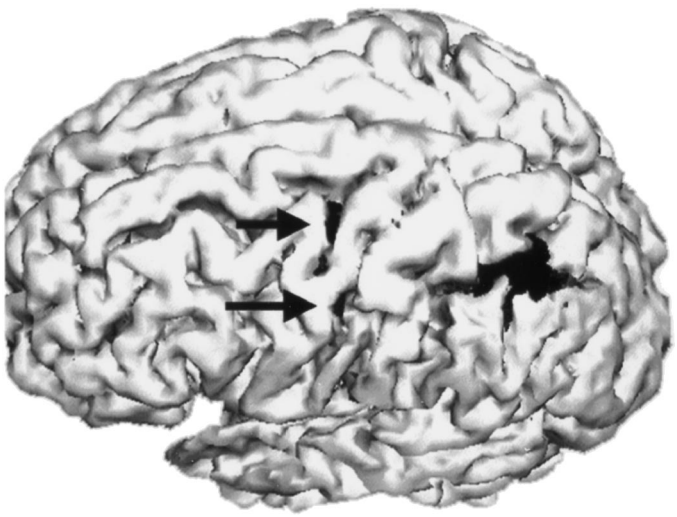

FIG. 6. Cortical areas for control of endpoint targeting. A comparison of the 2 target/width ratios across the 3 levels of movement difficulty was used to dissociate difficulty related to endpoint targeting (shown in black) from that primarily related to limb transport. Accurate endpoint targeting is associated with greater relative activity in the left motor cortex (bottom arrow), centered at the fundus of the central sulcus and extending into the adjacent precentral sulcus (top arrow) and also in the left intraparietal sulcus.

movement (Georgopoulos et al. 1986, 1995). With this, it is likely that in aiming situations in which more precise targeting is required, the motor cortex neurons are recruited to define this trajectory. We can only speculate as to whether a greater PET activation corresponds to more activity in a fixed number of neurons or whether a greater number of neurons is used to encode the intended movement. Given the covariation of movement velocity and force with ID, we expected that motor cortex activation would increase as force (velocity) increased. However, across ID conditions, the task type effect revealed a preferential activation in primary motor cortex for the lower-force (i.e., small type) aiming condition compared with the higher-force (i.e., large type) conditions. This comparison allowed a dissociation of the normal velocity/force covariation with ID and suggests that the primary motor cortex was preferentially activated in relation to the precise direction of force application and not simply the magnitude of force application.

It should be noted that the kinematic data analysis (MT and acceleration time) revealed an ID-by-task type interaction (locus in the 4.32 ID condition) not found to be significant in the complementary rCBF analysis. This is likely due to the fact that more data (all trials with each condition) were used in this analysis, whereas only the mean across all trials for each condition was used in the rCBF analysis, thereby reducing the statistical power for testing the interaction.

The recent real-time neural network model (VITE) proposed by Bullock and Grossberg (1988) to account for planned arm aiming movements uses the cell properties in the precentral motor cortex to provide continuous difference vector computations between the present position and the target position commands. With the use of this model, the speed-accuracy properties for aiming trajectories can be simulated. Consistent with our findings, this model suggests that where more precise targeting is required, the demands for this particular motor cortex cell computation would be greater.

In conclusion, our continuous aiming task is well constrained across the dimension of ID and well characterized by movement duration with the use of Fitts' law. The associated functional brain activation patterns capture most closely the multitude of automatic motor planning concerns, including visuomotor coordination, trajectory targeting, and compensation for limb dynamics. As a final note, it is interesting that for this unimanual aiming task, as ID increased, bilateral premotor activation was seen. The presence of bilateral motor planning areas for a unilateral task has implications for recovery from unilateral brain damage (e.g., stroke), where deficits in motor planning revealed by ipsilateral limb performance are more likely as task difficulty increases (e.g., Winstein and Pohl 1995).

The authors thank S. Hailes, K. Hamley, and B. Fisher for technical assistance, and Dr. Roger Woods for providing image analysis software.

This work was supported in part by grants from the Human Frontiers in Science Program, National Institute of Neurological Disorders and Stroke Grants NS-01568 and NS-33504 to S. Grafton, and The Foundation for Physical Therapy to C. Winstein.

Present addresses: S. Grafton, Dept. of Neurology, Emory University, Atlanta, GA 30303; P. Pohl, Center on Aging, The University of Kansas Medical Center, Kansas City, KS 66160.

Address for reprint requests: C. Winstein, Dept. of Biokinesiology and Physical Therapy, 1540 E. Alcazar St., CHP 155, Los Angeles, CA 90033.

Received 19 April 1996; accepted in final form 1 November 1996.

REFERENCES

ALEXANDER, G. E., CRUTCHER, M. D., AND DELONG, M. R. Basal ganglia thalamo-cortical circuits: parallel substrates for motor, oculomotor, ''prefrontal'' and ''limbic'' functions. *Prog. Brain Res.* 85: 119–146, 1990.

ASHE, J. AND GEORGOPOULOS, A. P. Movement parameters and neural activity in motor cortex and area 5. *Cereb. Cortex* 6: 590–600, 1994.

BASTIAN, A. J., MARTIN, T. A., KEATING, J. G., AND THACH, W. T. Cerebellar ataxia: abnormal control of interaction torques across multiple joints. *J. Neurophysiol.* 76: 492–509, 1996.

BOWER, J. M. Is the cerebellum sensory for motor's sake, or motor for sensory's sake? *Prog. Brain Res.* In press.

BROOKS, V. B., KOZLOVSKAYA, I. B., ATKIN, A., HORVATH, F. E., AND UNO, M. Effects of cooling dentate nucleus on tracking-task performance in monkeys. *J. Neurophysiol.* 36: 974–995, 1973.

BULLOCK, D. AND GROSSBERG, S. Neural dynamics of planned arm movements: emergent invariants and speed-accuracy properties during trajectory formation. *Psychol. Rev.* 95: 49–90, 1988.

CROSSMAN, E.R.F.W. AND GOODEVE, P. J. Feedback control of hand movements and Fitts' law (Original work published in 1963). *Q. J. Exp. Psychol. A Hum. Exp. Psychol.* 35: 251–278, 1983.

DECETY, J., PERANI, D., JEANNEROD, J., BETTINARDI, V., TADARY, B., WOODS, R., MAZZIOTTA, J. C., AND FAZIO, F. Mapping motor representations with PET. *Nature Lond.* 371: 600–602, 1994.

DEIBER, M.-P., PASSINGHAM, R. E., COLEBATCH, J. G., FRISTON, K. J., NIXON, P. D., AND FRACKOWIAK, R. S. J. Cortical areas and the selection of movement: a study with positron emission tomography. *Exp. Brain Res.* 84: 393–402, 1991.

FITTS, P. M. The information capacity of the human motor system in controlling the amplitude of movement. *J. Exp. Psychol.* 47: 381–391, 1954.

FITTS, P. M. AND PETERSON, J. R. Information capacity of discrete motor responses. *J. Exp. Psychol.* 67: 103–112, 1964.

FOX, P. T., MINTUN, M. A., RAICHLE, M. E., AND HERSCOVITCH, P. A noninvasive approach to quantitative functional brain mapping with $H_2{}^{15}O$ and positron emission tomography. *J. Cereb. Blood Flow Metab.* 4: 329–333, 1984.

FRISTON, K. J., FRITH, C. D., LIDDLE, P. F., AND FRACKOWIAK, R.S.J. Comparing functional (PET) images: the assessment of significant change. *J. Cereb. Blood Flow Metab.* 11: 690–699, 1991.

FU, Q.-G., SUAREZ, J. L., AND EBNER, T. J. Neuronal specification of direction and distance during reaching movements in the superior precentral premotor area and primary motor cortex in monkeys. *J. Neurophysiol.* 70: 2097–2116, 1993.

GEORGOPOULOS, A. P. Current issues in directional motor control. *Trends Neurosci.* 18: 506–510, 1995.

GEORGOPOULOS, A. P., DELONG, M. R., AND CRUTCHER, M. D. Relations between parameters of step-tracking movements and single cell discharge in the globus pallidus and subthalamic nucleus of the behaving monkey. *J. Neurosci.* 3: 1586–1598, 1983.

GEORGOPOULOS, A. P., SCHWARTZ, A. B., AND KETTNER, R. E. Neuronal population coding of movement direction. *Science Wash. DC* 233: 1416–1419, 1986.

GOODALE, M. A., MILNER, A. D., JAKOBSON, L. S., AND CAREY, D. P. A neurological dissociation between perceiving objects and grasping them. *Nature Lond.* 349: 154–156, 1991.

GRAFTON, S. T., ARBIB, M. A., FADIGA, L., AND RIZZOLATTI, G. Localization of grasp representations in humans by PET. 2. Observations versus imagination. *Exp. Brain Res.* 112: 103–111, 1996a.

GRAFTON, S. T., FAGG, A. H., WOODS, R. P., AND ARBIB, M. A. Cortical control of prehensile movements in humans. *Cereb. Cortex* 6: 226–237, 1996b.

GRAFTON, S. T., HUANG, S. C., MAHONEY, D. K., MAZZIOTTA, J. C., AND PHELPS, M. E. Analysis of optimal reconstruction filters for maximizing signal to noise ratios in PET cerebral blood flow studies (Abstract). *J. Nucl. Med.* 31: 865, 1990.

GRAFTON, S. T., MAZZIOTTA, J. C., WOODS, R. P., AND PHELPS, M. E. Human functional anatomy of visually guided finger movements. *Brain* 115: 565–587, 1992.

GRAFTON, S. T., WOODS, R. P., AND TYSZKA, J. M. Functional imaging of

procedural motor learning: relating cerebral blood flow with individual subject performance. *Hum. Brain Map.* 1: 221–234, 1994.

HERSCOVITCH, P., MARKHAM, J., AND RAICHLE, M. E. Brain blood flow measured with intravenous $H_2{}^{15}O$. I. Theory and error analysis. *J. Nucl. Med.* 24: 782–789, 1983.

JEANNEROD, M. The representing brain: neural correlates of motor intention and imagery. *Behav. Brain Sci.* 17: 187–245, 1994.

KEELE, S. Movement control in skilled motor performance. *Psychol. Bull.* 70: 387–403, 1968.

KEELE, S. Motor control. In: *Handbook of Perception and Performance*, edited by L. Kaufman, J. Thomas, and K. Boff. New York: Wiley, 1986, p. 1–60.

KELSO, J.A.S. Theoretical concepts and strategies for understanding perceptual-motor skill: from information capacity in closed systems to self-organization in open nonequilibrium systems. *J. Exp. Psychol. Gen.* 121: 260–261, 1992.

MACKENZIE, C. L., MARTENIUK, R. G., DUGAS, C., LISKE, D., AND EICKMEIER, B. Three-dimensional movement trajectories in Fitts' task: implications for control. *Q. J. Exp. Psychol. A Hum. Exp. Psychol.* 39: 629–647, 1987.

MAZZIOTTA, J. C., HUANG, S.-C., PHELPS, M. E., CARSON, R. E., MACDONALD, N. S., AND MAHONEY, K. A noninvasive positron computed tomography technique using oxygen-15-labeled water for the evaluation of neurobehavioral task batteries. *J. Cereb. Blood Flow Metab.* 5: 70–78, 1985.

MEYER, D. E., ABRAMS, R. A., KORNBLUM, S., WRIGHT, C. E., AND SMITH, J. E. K. Optimality in human motor performance: ideal control of rapid aimed movements. *Psychol. Rev.* 95: 340–370, 1988.

MILNER, T. E. AND IJAZ, M. M. The effect of accuracy constraints on three-dimensional movement kinematics. *Neuroscience* 35: 365–374, 1990.

NETER, J., WASSERMAN, W., AND KUTNER, M. H. *Applied Linear Statistical Models.* Boston, MA: Irwin, 1990.

OLDFIELD, R. C. The assessment and analysis of handedness: the Edinburgh inventory. *Neuropsychologia* 9: 97–113, 1971.

ORGOGOZO, J. M. AND LARSEN, B. Activation of the supplementary motor area during voluntary movement in man suggests it works as a supramotor area. *Science Wash. DC* 206: 847–850, 1979.

PICARD, N. AND STRICK, P. L. Motor areas of the medial wall: a review of their location and functional activation. *Cereb. Cortex* 6: 342–353, 1996.

PLAMONDON, R. A kinematic theory of rapid human movements. I. Movement representation and generation. *Biol. Cybern.* 72: 295–307, 1995a.

PLAMONDON, R. A kinematic theory of rapid human movements. II. Movement time and control. *Biol. Cybern.* 72: 309–320, 1995b.

POHL, P. S., WINSTEIN, C. J., AND FISHER, B. E. The locus of age-related movement slowing: sensory processing in continuous goal-directed aiming. *J. Gerontol. Psychol. Sci.* 51: 94–102, 1996.

PRABLANC, C., ECHALLIER, J. F., KOMILIS, E., AND JEANNEROD, M. Optimal response of eye and hand motor systems in pointing at a visual target. I. Spatial-temporal characteristics of eye and hand movements and their relationships when varying the amount of visual information. *Biol. Cybern.* 35: 113–124, 1979.

RAICHLE, M. E., MARTIN, W.R.W., AND HERSCOVITCH, P. Brain blood flow measured with intravenous $H_2{}^{15}O$. II. Implementation and validation. *J. Nucl. Med.* 24: 790–798, 1983.

RAO, S. M., BINDER, J. R., BANDETTINI, P. A., HAMMEKE, T. A., YETKIN, F. Z., JESMANOWIZ, A., LISK, L. M., MORRIS, G. L., MUELLER, W. M., ESTKOWSKI, L. D., WONG, E. C., HOUGHTON, V. M., AND HYDE, J. S. Functional magnetic resonance imaging of complex human movements. *Neurology* 43: 2311–2318, 1993.

REMY, P., ZILBOVICIUS, M., LEROY-WILLIG, A., SYROTA, A., AND SAMSON, Y. Movement- and task-related activations of motor cortical areas: a PET study. *Ann. Neurol.* 35: 19–26, 1994.

RIEHLE, A. AND REQUIN, J. Monkey primary motor and premotor cortex: single-cell activity related to prior information about direction and extend of an intended movement. *J. Neurophysiol.* 61: 534–549, 1989.

RIZZOLATTI, G., GENTILUCCI, M., FOGASSI, L., LUPPINO, G., MATELLI, M., AND PONZONI-MAGGI, S. Neurons related to goal-directed motor acts in inferior area 6 of the macaque monkey. *Exp. Brain Res.* 67: 220–224, 1987.

ROLAND, P. E., MEYER, E., SHIBASAKI, T., YAMAMOTO, Y. L., AND THOMPSON, C. J. Regional cerebral blood flow changes in cortex and basal ganglia during voluntary movements in normal human volunteers. *J. Neurophysiol.* 48: 467–480, 1982.

SCHMIDT, R. A., ZELAZNIK, H. N., HAWKINS, B., FRANK, J. S., AND QUINN, J. T. Motor-output variability: a theory for the accuracy of rapid motor acts. *Psychol. Rev.* 86: 415–451, 1979.

SCHNEIDER, K., ZERNICKE, R. F., SCHMIDT, R. A., AND HART, T. J. Changes in limb dynamics during the practice of rapid arm movements. *J. Biomech.* 22: 805–817, 1989.

SCHWARTZ, A. B., KETTNER, R. E., AND GEORGOPOULOS, A. P. Primate motor cortex and free arm movements to visual targets in three-dimensional space. I. Relations between single cell discharge and direction of movement. *J. Neurophysiol.* 8: 2913–2927, 1988.

SHIBASAKI, H., SADATO, N., LYSHKOW, H., YONEKURA, Y., HONDA, M., NAGAMINE, T., SUWAZONO, S., MAGATA, Y., IKEDA, A., MIYAZAKI, M., FUKUYAMA, H., ASATO, R., AND KONISHI, J. Both primary motor cortex and supplementary motor area play an important role in complex finger movements. *Brain* 116: 1387–1398, 1993.

SMITH, J. L. AND ZERNICKE, R. F. Predictions for neural control based on limb dynamics. *Trends Neurosci.* 10: 123–128, 1987.

STEPHAN, K. M., FINK, G. R., PASSINGHAM, R. E., SILBERSWEIG, D., CEBALLOS-BAUMANN, A. O., FRITH, C. D., AND FRACKOWIAK, R.S.J. Imaging the execution of movements. *J. Neurophysiol.* 73: 373–386, 1995.

TAIRA, M., MINE, S., GEORGOPOULOS, A. P., MURATA, A., AND SAKATA, H. Parietal cortex neurons of the monkey related to the visual guidance of hand movement. *Exp. Brain Res.* 83: 29–36, 1990.

TALAIRACH, J. AND TOURNOUX, P. *Co-Planar Stereotaxic Atlas of the Brain.* New York: Thieme, 1988.

TANJI, J. The supplementary motor area in the cerebral cortex. *Neurosci. Res.* 19: 251–268, 1994.

TYSZKA, J. M., GRAFTON, S. T., CHEW, W., WOODS, R. P., AND COLLETTI, P. M. Parcellation of mesial frontal motor areas during ideation and movement using functional magnetic resonance imaging at 1.5 Tesla. *Ann. Neurol.* 35: 746–749, 1994.

WALLACE, S. A. AND NEWELL, K. M. Visual control of discrete aiming movements. *Q. J. Exp. Psychol. A Hum. Exp. Psychol.* 35: 311–321, 1983.

WINSTEIN, C. J. AND POHL, P. S. Effects of unilateral brain damage on the control of hand aiming movements in humans. *Exp. Brain Res.* 105: 163–174, 1995.

WOODS, R. P., CHERRY, S. R., AND MAZZIOTTA, J. C. Rapid automated algorithm for aligning and reslicing PET images. *J. Comput. Assist. Tomogr.* 115: 565–587, 1992.

WOODS, R. P., IACOBONI, M., GRAFTON, S. T., AND MAZZIOTTA, J. C. Three-way analysis of variance. In: *Quantification of Brain Function Using PET*, edited by R. Meyers, V. Cunningham, and D. Bailey. New York: Academic, 1996, p. 353–358.

WOODS, R. P., MAZZIOTTA, J. C., AND CHERRY, S. R. MRI-PET registration with automated algorithm. *J. Comput. Assist. Tomogr.* 17: 536–546, 1993a.

WOODS, R. P., MAZZIOTTA, J. C., AND CHERRY, S. R. Automated image registration. In: *Quantification of Brain Function. Tracer Kinetics and Image Analysis in Brain PET*, edited by K. Vemera, N. A. Lassen, T. Jones, and I. Kanno. Amsterdam: Excerpta Medica, 1993, p. 391–398.

WOODWORTH, R. S. The accuracy of voluntary movement. *Psychol. Rev.* 3: 2, whole No. 13, 1899, p. 1–114.

WORSLEY, K. J., EVANS, A. C., MARRETT, S., AND NEELIN, P. A three-dimensional statistical analysis for CBF activation studies in human brain. *J. Cereb. Blood Flow Metab.* 12: 900–918, 1992.

ZILLES, K., SCHLAUG, G., GEYGER, S., LUPPINO, G., MATELLI, M., QU, M., AND SCHORMANN, T. Anatomy and transmitter receptors of the supplementary motor areas in the human and non human primate brain. In: *Advances in Neurology: Supplementary Sensorimotor Area*, edited by O. Lueders. Philadelphia, PA: Lippincott-Raven, 1996, vol. 70, p. 29–43.